



Sandpile-based model for capturing magnitude distributions and spatiotemporal clustering and separation in regional earthquakes

Rene C. Batac¹, Antonino A. Paguirigan Jr.¹, Anjali B. Tarun¹, and Anthony G. Longjas²

¹National Institute of Physics, University of the Philippines Diliman 1101 Quezon City, Philippines

²St. Anthony Falls Laboratory, University of Minnesota, 2 Third Ave. SE, Minneapolis MN 55414, USA

Correspondence to: R.C. Batac (rbatac@nip.upd.edu.ph)

Abstract. We propose a cellular automata model for earthquake occurrences patterned after the sandpile model of self-organized criticality (SOC). By incorporating a single parameter describing the probability to target the most susceptible site, the model successfully reproduces the statistical signatures of seismicity. The energy (magnitude) distributions closely follow power-law probability density functions (PDFs) with scaling exponent $-5/3$, consistent with the expectations of the Gutenberg-Richter (GR) law, for a wide range of the targeted-triggering probability values; this suggests that SOC mechanisms are still present in the model despite the introduction of the targeted triggering. Additionally, for targeted triggering probabilities within the range 0.004-0.007, we observe spatiotemporal distributions that show bimodal behavior, which is not observed previously for the original sandpile. For this critical range of values for the probability, model statistics show remarkable comparison with long-period empirical data from earthquakes from different seismogenic regions. The proposed model has key advantages, foremost of which is the fact that it simultaneously captures the energy, space, and time statistics of earthquakes by just introducing a single parameter, without disrupting the SOC properties of the sandpile grid. We believe that the critical-targeting probability is a key requirement for SOC, as it parametrizes the memory that is inherently present in earthquake-generating regions.

1 Introduction

The sandpile model, introduced as a representative system for illustrating self-organized criticality (SOC) (Bak, Tang, Wiesenfeld, 1987), has opened up new avenues for the use of discrete cellular automata (CA) models in capturing the salient features of many systems in nature (Olami, Feder, Christensen, 1992; Drossel and Schwabl, 1992; Malamud and Turcotte, 2000; Piegari et al., 2006; Juanico et al., 2008). Seismicity, which is rife with power-law statistical distributions (Saichev and Sornette, 2006), is an interesting test case for such approaches. Despite the complexity of the processes in the earth's crust that limit our ability for accurate, short-term prediction of events, it is worth noting that many statistical features of seismicity, as obtained from substantially complete earthquake records, can be recovered using simple CA models.

One of the earliest attempts for sandpile-based modelling of earthquake distributions is by Bak and Tang (1989), who used a two-dimensional sandpile to show the power-law Gutenberg-Richter (GR) distributions of earthquake energies (Gutenberg and Richter, 1954). Subsequent authors also noted that the simple sandpile produces power-law distributions of earthquake waiting



times upon introducing a threshold magnitude (Paczuski et al., 2005). Additional parameters have been introduced in the model to account for other features of seismicity. Ito and Matzusaki (1990) introduced aftershock triggering to the sandpile model to recover the aftershock frequencies and the hypocenter distributions, which also follow power-law decays. To represent a scale invariant distribution of earthquake faults, Barriere and Turcotte (1991) incorporated a power law distribution of box sizes in the CA model, and recovered not only the GR distribution but the occurrence of foreshocks. On the other hand, Steacy et al. (1996) investigated the effect of a heterogeneous strength distribution and found that the power-law exponent of the magnitude distribution is dependent on the degree of the heterogeneity. Inspired by the sandpile design, Olami, Feder, Christensen (1992) used a CA implementation of the earlier Burridge-Knopoff model Burridge and Knopoff (1967) that incorporates dissipative terms and inhomogeneous energy redistribution rules to capture key elements of seismicity, along with foreshocks and aftershocks Hergarten and Neugebauer (2002).

Needless to say, introducing additional parameters, while being able to account for more realistic scenarios on the ground, result in the possible loss of SOC characteristics. Moreover, we observe that previous implementations are not able to replicate the regimes of spatiotemporal clustering and separation in earthquakes. In this work, we aim to strengthen the association between earthquakes and SOC by attempting to recover magnitude, space, and time distributions of seismicity using a sandpile with minimal additional parameters. The modified sandpile we implemented contains a probability to target the site with highest susceptibility. Upon scanning through a wide range of values for this parameter, we observe that the system preserves the SOC characteristics and the GR exponents. At some characteristic values of the targeted triggering probability, the resulting distributions in space and time, which show strong clustering and separation (Batac and Kantz, 2014; Batac, 2015), are also captured. The fact that the model replicates earthquake statistics simultaneously in magnitude, space, and time dimensions with minimal additional parameters make the model more truthful to the original sandpile design, presenting a clear association with seismicity and SOC. The probability for targeted triggering is deemed to parametrize the memory in earthquake-generating mechanisms in different seismogenic regions.

2 Model Specifications

The model utilizes a two-dimensional space discretized into a grid of $L \times L$ cells arranged in a square lattice. The cells contain continuous-valued information states σ representing the local measure of susceptibility to rupture. At time $t = 0$, the states are initialized to have values within $[0, \sigma_{\max})$, where, in this case, we set $\sigma_{\max} = 1.0$ as the relative measure of the rupture threshold.

The dynamical evolution of the grid is guided by rules patterned after the Zhang sandpile that uses continuous-valued states (Zhang, 1989). We choose an asynchronous update rule, such that every discrete time step, the grid is triggered by adding a constant value ν to a chosen location (x, y) , $\sigma(x, y, t + 1) \rightarrow \sigma(x, y, t) + \nu$. The asynchronicity is deemed to represent the nonuniformity of crustal motion that drives the accumulation of elastic potential energy at faults. Moreover, the model introduces a targeted triggering probability p that the most susceptible site, i.e. the site with the highest σ value in the grid, will receive the driving term ν . Triggering is therefore applied to the most susceptible site with probability p , and to a randomly



chosen site with probability $1 - p$. The value of p represents a memory term, and parameterizes the tendency of fracture to occur at more susceptible locations along an earthquake generating zone.

In the event when a local cell matches or exceeds the threshold σ_{\max} , the local region is deemed to rupture. As in the sandpile and OFC models, no new trigger is added to the system during such events; instead, the stress from the collapsing site are transferred to the four nearest neighbors in the grid, $\sigma(x \pm 1, y \pm 1, t) \rightarrow \sigma(x \pm 1, y \pm 1, t) + \frac{1}{4}\sigma(x, y, t)$, leading to the relaxation of the original site, $\sigma(x, y, t) \rightarrow 0$. Such relaxations may produce a cascade of subsequent stress redistributions and relaxations in the grid when one or more of the neighbors are themselves driven to the threshold. The number of affected sites in the grid, A , is used as a proxy for the actual energy or magnitude of the relaxation event.

Prior calibrations show that $\nu = 10^{-3}$ produce power-law avalanche-size distributions comparable to the GR law, and that $t_{\max} = \{1, 4, 16\} \times 10^7$ iterations, where the first 10% are neglected for transient behavior, produces substantial number of avalanche events for $L = \{256, 512, 1024\}$ grids, respectively. We investigated the case of different targeted triggering probabilities $p = \{0, 1 \times 10^k, 5 \times 10^k, 1\}$, where the integer k is from -5 to -1 to scan a wide range of possible system behaviors. For each of the p values, we track all nonzero A_i and their avalanche origins and occurrence times (x_i, y_i, t_i) , where i denotes the temporal index of occurrence of an event. The spatial and temporal separations of successive events, $R_i = [(x_i - x_{i-1})^2 + (y_i - y_{i-1})^2]^{1/2}$ and $T_i = t_i - t_{i-1}$, are computed, and the probability density functions (PDFs) of all A , R , and T are plotted.

Finally, as a way of comparison and verification, we compare the model statistics with those obtained from actual earthquake catalogs from Japan (JP), Philippines (PH), and Southern California (SC), as investigated in a previous work by Batac and Kantz (2014). The JP records are obtained from the Japan University Network Earthquake Catalog (JUNEC), with approximately 137,000 events from July 1985-December 1998; the PH earthquakes are composed of 70,000+ events from 1973 to 2012, as obtained from the Preliminary Determination of Earthquakes (PDE) Catalog; while the SC records are from the Southern California Earthquake Catalog (SCEC) containing 516,000+ events from 1982 to 2012 (events due to man-made activities are removed). Apart from the similarity in the trends, we attempt to calibrate model parameters to fit the data, and interpret the obtained calibration parameters.

3 Results

Figure 1(a) shows the avalanche size probability density functions (PDFs) for the different values of the targeted triggering probability p . For the broad range of p values considered, the distributions are found to be comparable to a power-law $A^{-\alpha}$ with $\alpha = 1.6$. The obtained exponent is within the same order as those obtained using similar asynchronous updating models (Paguirigan et al., 2015), and is significantly larger than in synchronous (i.e., parallel updating) cases (Lübeck, 1997). The fact that the distributions are almost similar regardless of the value of p indicates that the targeted triggering probability has minimal effect on the avalanching mechanism of the grid, such that the system preserves the SOC characteristics of the original pile. In contrast, the OFC model, for example, tends to lose the universality of the exponents upon the introduction of nonconservation (Olami, Feder, Christensen, 1992). By introducing p , therefore, we believe that the model is more faithful to

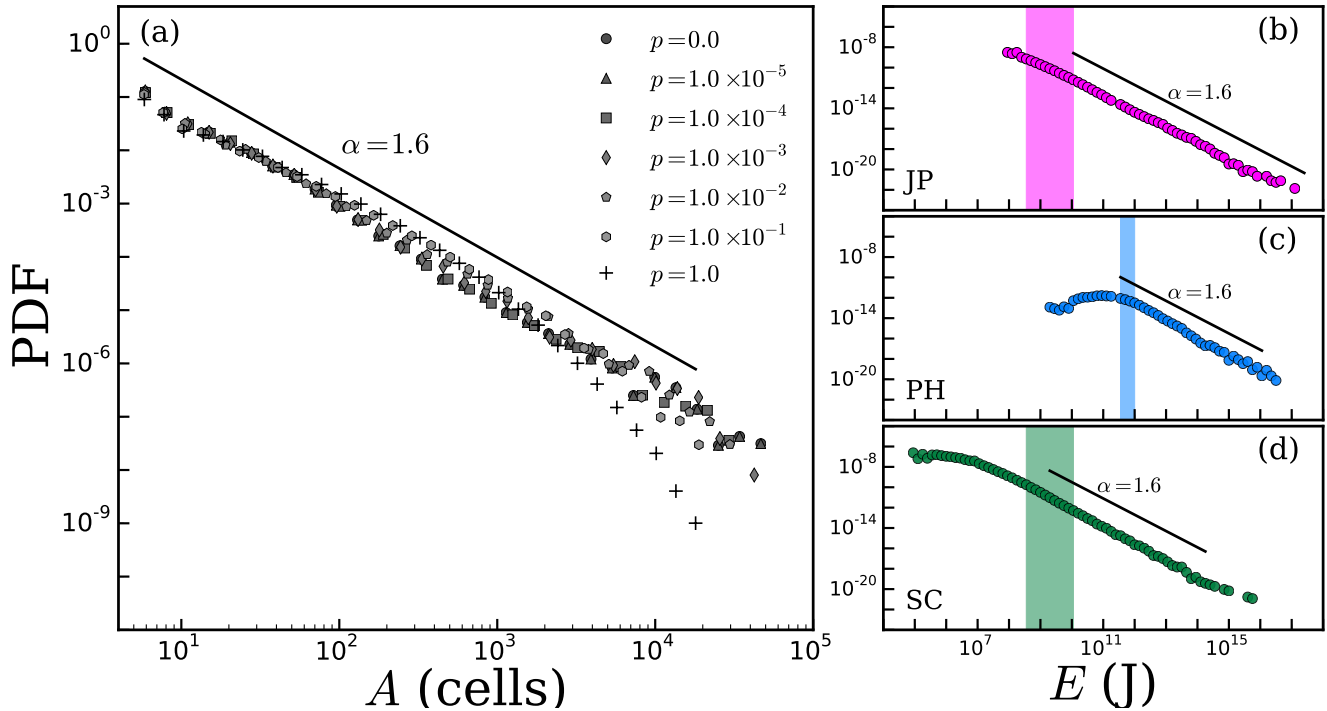


Figure 1. Avalanche size and earthquake energy PDFs. For all figures, lines corresponding to the power-law trend with exponent $\alpha = 1.6$ are provided as guides to the eye. (a) Model results show similar behaviors despite the large differences in p , signifying the preservation of SOC characteristics of the grid. The obtained power-law distributions are comparable to the power-law trends in the energy distributions from (b) Japan, JP; (c) Philippines, PH; and (d) Southern California, SC. In (b)-(d), the horizontal axes scales are preserved; shaded regions denote energy values with substantial completeness, which will be used for subsequent analyses.

the actual mechanisms observed in the generation of earthquakes, which, despite regional differences, produce universal GR distributions.

In Figure 2(a), we observe that the original sandpile $p = 0$ produces unimodal statistics, whose tails decay towards the largest possible distance $\sqrt{2}L$ in the finite grid. The simple sandpile, therefore, is not capable of replicating the observed earthquake separation distance distributions, which are found to exhibit bimodality due to the difference in the characteristic times of the correlated aftershock sequences and the independent mainshocks (Baiesi and Paczuski, 2004; Zaliapin et al., 2008; Touati et al., 2009; Batac and Kantz, 2014).

In Figure 3(a), the results for $L = 256$ and $t_{\max} = 10^7$ iterations, show the expected shift of the tail cutoff for shorter T as p is increased; triggering the highly-susceptible sites will more likely result in a new avalanche event, thereby shortening the average waiting time. However, for the threshold $A_{th} = 50$ used, we have not seen the power-law regimes due to the short t_{\max} . In the calibration with real-world data shown in Figure 3(b)-(d), we used the same $p^* = 0.007$, and obtained similarities only for the largest grids and longest iteration times, $L = 1024$ and $t_{\max} = 16 \times 10^7$. Calibration in time is made such that 1 iteration

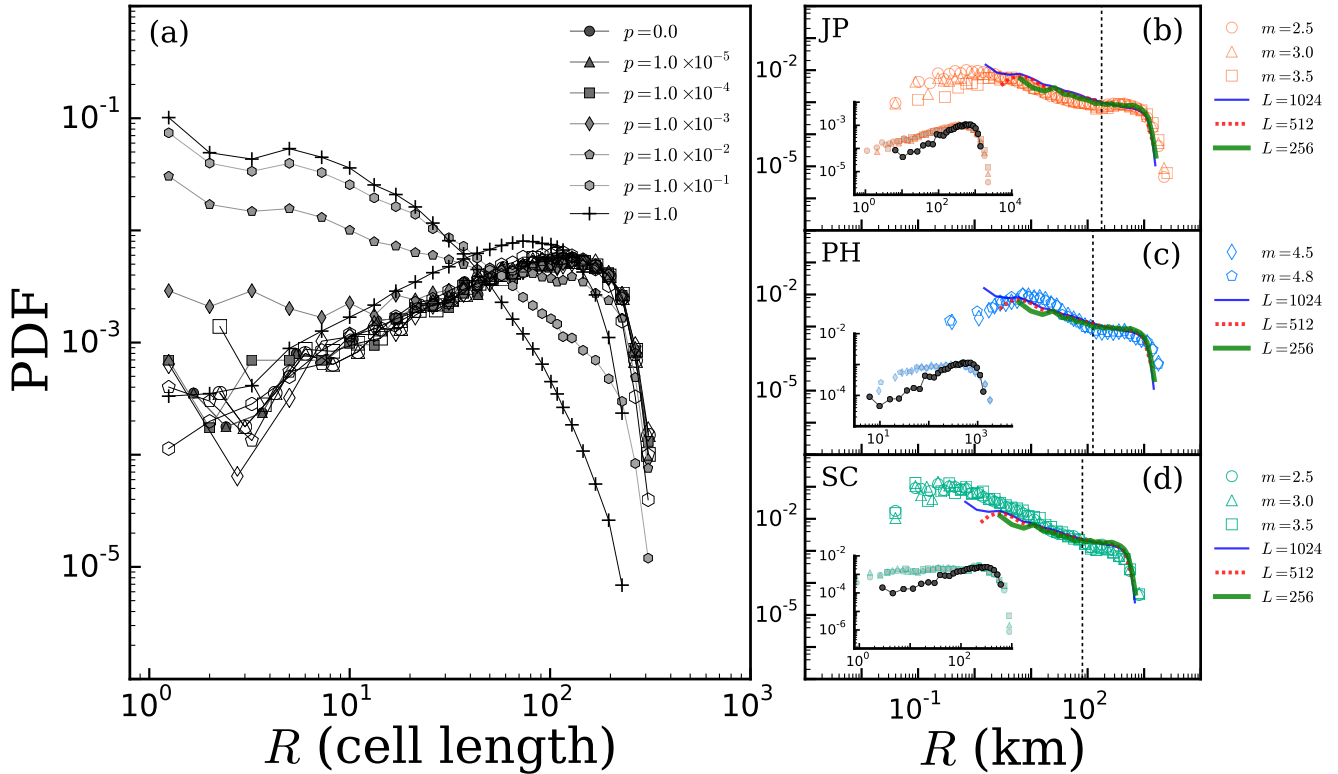


Figure 2. (Color online) Interevent distance statistics of model, rescaled to correspond to actual earthquake separation distance data. (a) For a $L = 256$ grid, higher p results in the preponderance of short- R values. The trends of the model closely mimic those of the data for (b) JP, (c) PH, and (d) SC, where calibration was done by comparing the modes of the shuffled sequences, as shown in the insets of (b)-(d). Larger grids in (b)-(d) result in the capability to replicate the shorter R regimes. The crossover point between data and shuffled statistics R^* are marked by broken lines. The R^* will be used for obtaining conditional distributions of interevent times.

is roughly 0.1 min, corresponding to the ratio of the total length of time considered (in minutes) and the number of iterations used. The appropriate A_{th} , which is the model equivalent of the threshold magnitude m for the data, is found by comparing the power-law trends. We obtained $A_{th} = 5$ for JP, $A_{th} = 10^5$ for PH, and $A_{th} = 5 \times 10^3$ for SC. The geographical extent, level of background activity, recording sensitivity and data completeness all play a factor in the number of events recorded in the region; as such, there is no one-on-one correspondence between A_{th} and m .

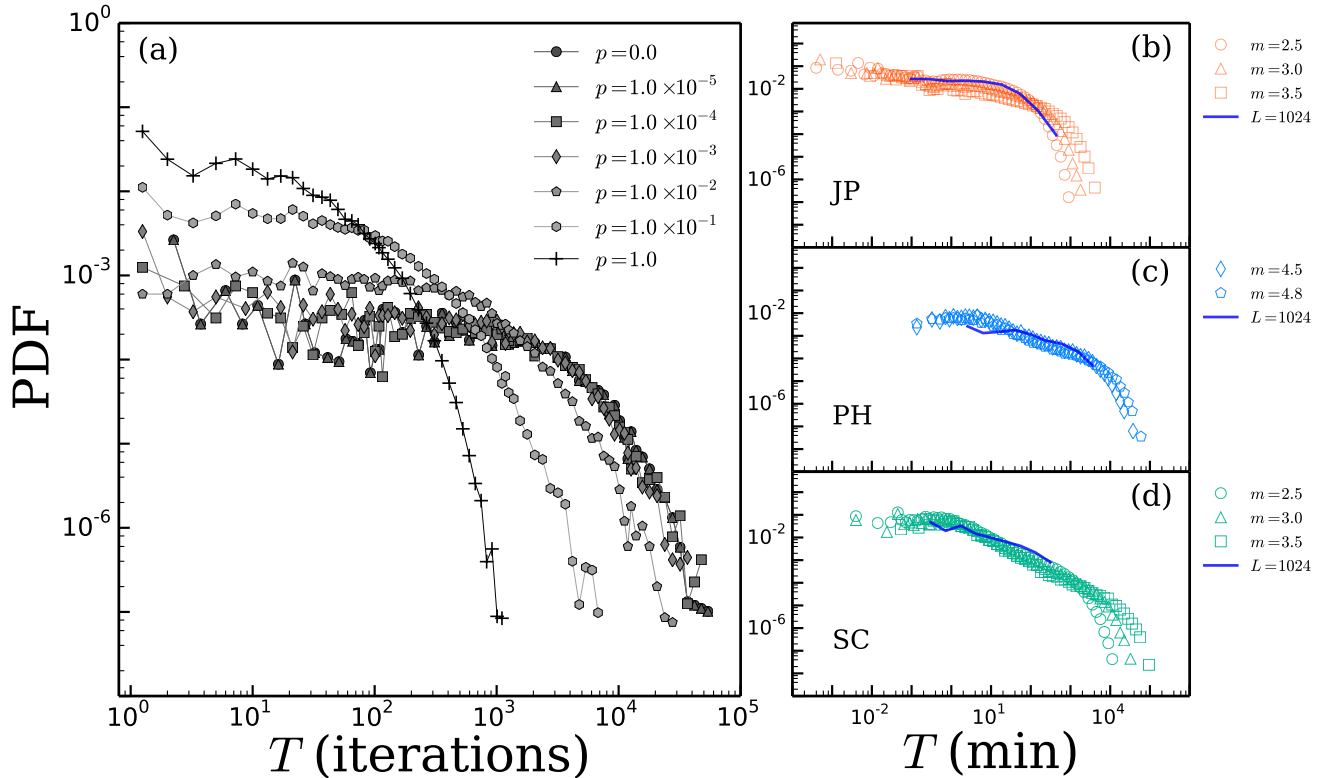


Figure 3. (Color online) Interevent time statistics of model, rescaled to correspond to actual earthquake waiting time data. (a) For a $L = 256$ grid, higher p results in the shift of the distribution to shorter T values. To obtain substantial power-law regimes, we used the results for the $L = 1024$ grid to replicate the waiting time statistics of (b) JP, (c) PH, and (d) SC. By setting the unit iteration time as around 0.1 min, we found that the appropriate threshold magnitudes that will result in comparable power-law decays are (b) $A_{th} = 5$ for JP; (c) $A_{th} = 10^5$ for PH; and (d) $A_{th} = 5 \times 10^3$ for SC.

4 Discussion

4.1 Energy Distributions and the Gutenberg-Richter Law

The GR law, which is usually presented in terms of the moment magnitudes M_w and as a complementary cumulative distribution function (CCDF), can be shown to be equivalent to an energy E CCDF that behaves as $E^{-2/3}$ from the definition of m and by assuming $b = 1$, which is the case for most complete records. By noting that the CCDF is effectively an integral of the PDF, the earthquake energy PDF will then behave as $E^{-5/3}$, which is comparable to the model-obtained exponents. In Figure 1(b)-(d), similar power-law trends have been obtained for the JP, PH, and SC records, which have different levels of catalog completeness, as indicated by the extent of the power-law regimes. To minimize the problems associated with the inherent incompleteness of smaller-energy events (Zaliapin and Ben-Zion, 2015), we impose a threshold magnitude (energy)



m for succeeding analyses such that earthquake events with magnitudes lower than m are dropped from consideration. The range of such magnitudes considered, which are well within the power-law regimes of the plots, are shaded in Figure 1(b)-(d): $m \in [2.5, 3.5]$ for JP and SC and $m \in [4.5, 4.8]$ for PH.

It is worth emphasizing that similar power-law trends result from the introduction of the parameter p , regardless of how large its relative value is. In fact, Figure 1(a) shows that even for the extreme case of a biased sandpile, $p = 1$, the PDF still follows comparable trends as with other p values. The fact that the model can replicate the energy statistics is a vital first requirement for any discrete model of earthquakes. Our proposed model has the additional advantage of faithfully preserving SOC mechanisms, which are believed to be exhibited by seismicity in the first place.

4.2 Spatial Separation of Earthquake Events

In the original asynchronous sandpile models, one only recovers unimodal statistics for interevent distances. This is due to the stochastic nature of the triggering: the next location to be perturbed is drawn from an oftentimes uniform distribution, i.e. all sites are likely to be triggered next. The same cannot be said of earthquakes: after the release of elastic potential energy at a fault location, the subsequent crustal motion may tend to favor other fractures near the vicinity of the earlier event, to release the remaining stored energy.

This simple illustration led us into the introduction of p , which is directly affecting the spatial distribution of events in the grid. The parameter p is just the probability to target the most susceptible site in the lattice, unlike previous implementations that actually bias the next targeting location within the vicinity of the previous avalanche (Ito and Matzusaki, 1990). Without such biasing, however, the replication of the short- R regimes is not guaranteed. Interestingly, however, the plots in Figure 2(a) show increased probability of occurrence of the short- R distances upon introducing nonzero p . From this, we can deduce that the most susceptible sites in the lattice are most likely to be found within the vicinity of a previous large avalanche, a fact that was not exploited by earlier similar models. In fact, in the biased case $p = 1$, we recovered unimodal statistics, as shown in Figure 2(a), albeit at a shorter characteristic distance; for the $L = 256$ grid, the average location of the most susceptible site from the previous avalanche origin was obtained to be around 21 cell lengths. Midway between these two extremes ($p = 0$ for the original, and $p = 1$ for the completely biased sandpile), we can find a suitable value of p where reasonable comparison with empirical data can be obtained.

Without any form of spatial clustering, the characteristic separation distance is limited by the finite system size. Rescaling is therefore conducted by comparing the characteristic sizes (modes) of the memoryless cases of the model ($p = 0$) and the data (shuffled sequence). Scanning through the possible p values, we observe that the best fit between data and model is obtained for $p^* \approx 0.004 - 0.007$. In Figure 2(b)-(d), we find that the rescaled model statistics for $p = 0.007$ show good agreement with interevent distances from the three seismogenic regions. Because of the nature of the rescaling procedure used, model statistics all collapse toward the exponential finite-size scaling regime at the tails of the distributions. Additionally, larger grid sizes result in better resolution, such that shorter R regimes are captured better. For the largest grids used ($L = 1024$), we find that the calibration for a unit cell length are: 1.3 km for JP, 1.2 km for PH, and 0.5 km for SC.



4.3 Temporal Separation of Earthquake Events

The temporal separation of aftershocks and mainshocks that have different characteristic waiting times is an intuitive result that is both well-known and more widely studied (Zaliapin et al., 2008; Touati et al., 2009; Batac and Kantz, 2014; Batac, 2015). In comparing model and empirical temporal interevent statistics, however, one does not have the similar advantage of having a finite “space” for comparison. The goal of rescaling in time is to recover the shortest T first; the longest T will be recovered if the model is allowed to run for longer times. Additionally, in rescaling the time, one should take into account the fact that the earthquake record is thresholded by m , effectively lengthening the average time between the occurrence of two events. Previous sandpile-based models suggest that the waiting time distribution will be Poisson distributed when all the events are considered, but will begin to show power-law characteristics upon thresholding (Paczuski et al., 2005; Juanico et al., 2008).

Such procedure was implemented in Figure 3(b)-(d) for the same parameters ($p^* = 0.007$, $L = 1024$). The results are not easily appreciated due to the finite size of the grid and finite iteration times, which limits the possibility for recovering the very long waiting times as in the data. However, the results are better highlighted by applying the same procedure by Batac and Kantz (2014) of finding the conditional PDFs of T subject to its corresponding R . For the same $p^* = 0.007$ and $L = 1024$, and for the A_{th} found that matches the data for each of the regions considered, we plot in Figure 4 the PDFs of $T_{in} = \{T|R \leq R^*\}$ and $T_{out} = \{T|R > R^*\}$ for both data (a)-(c) and model (d)-(f), where the R^* values are the intersections of the interevent distances of the data and the shuffled sequences denoted by the broken lines in Figure 2(b)-(d).

The PDFs of T_{in} and T_{out} differ significantly from that of the total T , with T_{in} showing higher probabilities of having shorter T values, suggesting a strong dependence among the interevent properties in space and time (Livina et al., 2005). This conditional distribution therefore quantifies the spatiotemporal clustering observed in earthquakes, particularly among aftershock sequences that result from the correlated mechanisms. As expected, the T_{out} distributions do not coincide due to the limited iteration length of the model; however, it is particularly interesting to note that the calibrated T_{in} statistics of model and data show comparable trends, especially for shorter waiting times, as shown in the insets of Figure 4(d)-(f). The T_{in} statistics has been shown to correspond nicely with the statistics of aftershocks, as shown in studies of fresh aftershock statistics from empirical data (Batac, 2015). This suggests that the correlated mechanisms in actual earthquake systems that produce the T_{in} distributions is also present in the model.

4.4 Model Advantages and Insights on Empirical Modeling

The discrete model presented in the work has to be benchmarked with respect to other, earlier models that were inspired by the sandpile. One key advantage of the proposed approach is the fact that it is a sandpile, with the rules closely following the Bak-Tang-Wiesenfeld (BTW) design (Bak, Tang, Wiesenfeld, 1987) for asynchronous driving and nearest-neighbor redistribution rules, without introducing dissipative parameters, which can sometimes lead to the loss of SOC characteristics (Olami, Feder, Christensen, 1992). The introduction of continuous states for each of the cell allows for flexibility in calibration, as discussed above. Apart from the parameter p , the model retains the simplicity and the SOC nature of the original sandpile grid.

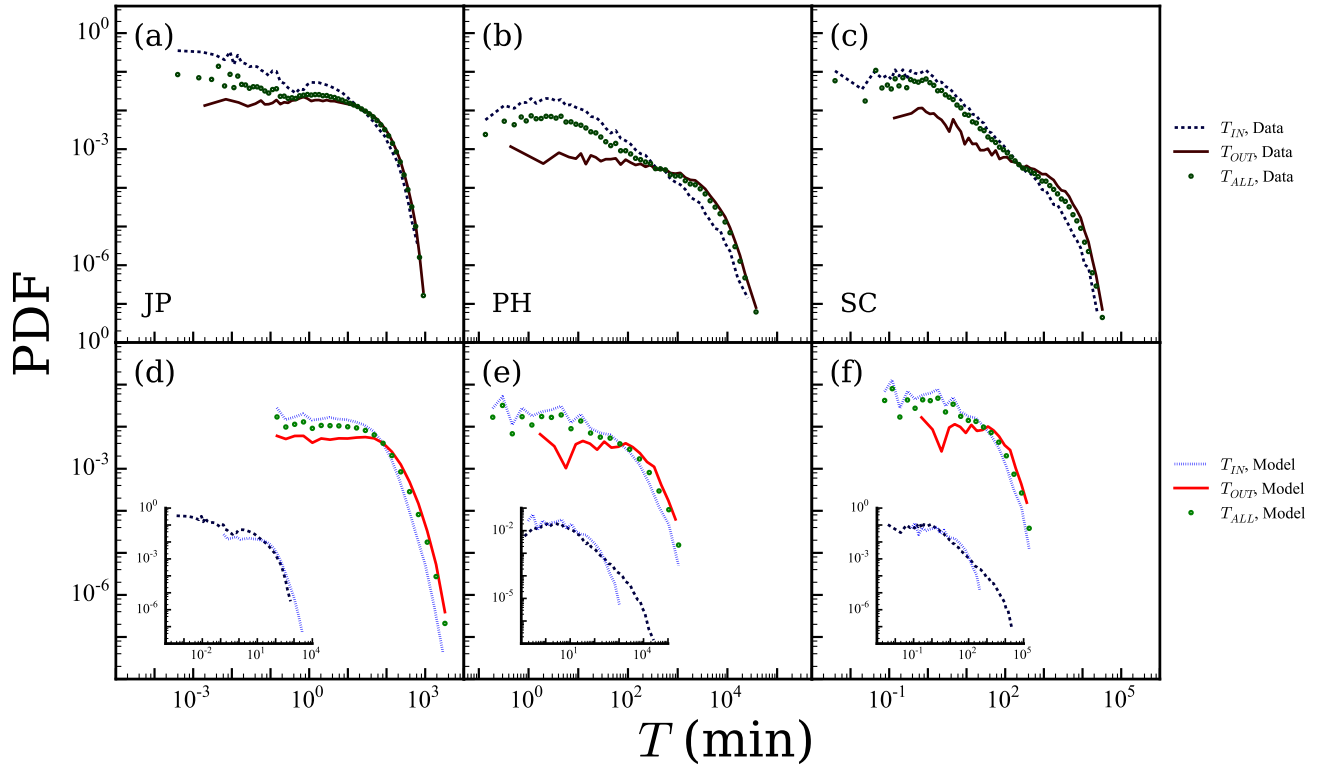


Figure 4. (Color online) Conditional PDFs of T_{in} and T_{out} for (a)-(c) earthquake data and (d)-(f) corresponding calibrated model results, plotted with the total PDF of all T . Nearby (Far away) events have higher (lower) chance of having short waiting times and lower (higher) chance of having long waiting times. The insets of (d)-(f) show that the T_{in} of model and rescaled data have significant overlap, signifying the similarities in their correlated origins.

Introducing the parameter p into the sandpile driving is a straightforward way of incorporating memory into the system. This simple parameter holds a distinct advantage over other models that introduced additional parameters, because it spans a wide range of possible statistical distributions in energy (avalanche size), space, and time, without actually biasing the location of the next triggering event. We believe that this parameter, which, for earthquakes, show comparable statistics for the range

5 $p^* \approx 0.004 - 0.007$, may be introduced in other sandpile-based models of other events in nature deemed to be showing SOC characteristics.

Being a single parameter, the correspondence between p and actual properties of the earthquake-generating system may be difficult, if not impossible, to ascertain. At best, we may think of p as a combined effect of many different factors on the ground that lead to the preferential triggering of a location.



5 Conclusions

In summary, we have presented a simple cellular automata model inspired by the original sandpile model of self-organized criticality (SOC). The model avoids introducing biased rules, and instead incorporates a probability of targeting the most susceptible site in the grid, reminiscent of the assumed fracture mechanism of actual earthquake systems. Within a small range of values $p^* \approx 0.004 - 0.007$, we have observed that the model statistics show good agreement with empirical distributions of earthquake energies in energy, space, and time. The fact that the simple targeted triggering probability simultaneously recovers these important statistical features of earthquakes is a simple yet novel concept that has been overlooked by previously-proposed discrete models of seismicity.

The work has also uncovered an important property of the sandpile grid: the most susceptible sites lie within the vicinity of a previous large avalanche event. Previous sandpile-based models that synchronously update all lattice sites, or those that asynchronously update at random locations, are not able to exploit this important property, preventing the possibility of directly modelling earthquakes using the sandpile paradigm. More importantly, we have shown that the introduction of such a targeting probability stays true to the SOC nature of the sandpile grid, in contrast with other models where the SOC properties are lost. With the proposed model, the association between earthquakes and SOC can be further investigated. The targeted triggering probability, which is shown to preserve the SOC characteristics, may also be introduced to better capture the spatiotemporal properties of other systems in the real world that are believed to be exhibiting SOC.

Author contributions. R.C.B. devised the model and A.A.P.J. run large-scale simulations. R.C.B. and A.B.T. wrote the paper. A.G.L. and A.B.T. provided the empirical data and model comparisons. A.B.T. and A.A.P.J. conducted statistical goodness-of-fit tests.

Acknowledgements. The authors would like to acknowledge financial support from the University of the Philippines Diliman (UPD) Office of the Vice Chancellor for Research and Development (OVCRD) through a PhD Incentive Award with project title “Quantifying the clustering characteristics of complex, self-organizing systems in nature and society.” A.A.P.J. acknowledges the Department of Science and Technology (DOST) for his Advanced Science and Technology Human Resources Development Program (ASTHRDP) scholarship.



References

- Baiesi, M. and Paczuski, M.: Scale-free networks of earthquakes and aftershocks, *Phys. Rev. E*, 69, 066106, doi:10.1103/PhysRevE.69.066106, 2004.
- Bak, P. and Tang, C.: Earthquakes as a Self-Organized Critical Phenomenon, *J. Geophys. Res.*, 94, 15635-15637, doi:10.1029/JB094iB11p15635, 1989.
- 5 Bak, P., Tang, C., and Wiesenfeld, K.: Self-organized criticality - An explanation of the $1/f$ noise, *Phys. Rev. Lett.*, 59, 381, doi:10.1103/PhysRevLett.59.381, 1987.
- Barriere, B. and Turcotte, D. L.: A scale-invariant cellular automata model for distributed seismicity, *Geophys. Res. Lett.*, 18, 2011-2014, doi:10.1029/91GL02415, 1991.
- 10 Batac, R. C.: Statistical Properties of the Immediate Aftershocks of the 15 October 2013 Magnitude 7.1 Earthquake in Bohol, Philippines, *Acta Geophysica*, 64, 15-25, doi:10.1515/acgeo-2015-0054, 2015.
- Batac, R. C. and Kantz, H.: Observing spatio-temporal clustering and separation using interevent distributions of regional earthquakes, *Nonlin. Proc. Geophys.*, 21, 735-744, doi:10.5194/npg-21-735-2014, 2014.
- Burridge, R. and Knopoff, L.: Model and theoretical seismology, *B. Seismol. Soc. Am.*, 57, 341, 1967.
- 15 Drossel, B. and Schwabl, F.: Self-organized critical forest-fire model, *Phys. Rev. Lett.*, 69, 1629-1632, doi:10.1103/PhysRevLett.69.1629, 1992.
- Gutenberg, B. and Richter, C. F.: *Seismicity of the Earth and Associated Phenomena*, 2nd ed., Princeton, N.J.: Princeton University Press, 1954.
- Hergarten, S. and Neugebauer, H. J.: Foreshocks and Aftershocks in the Olami-Feder-Christensen Model, *Phys. Rev. Lett.*, 88, 238501, doi:10.1103/PhysRevLett.88.238501, 2002.
- 20 Ito, K. and Matsuzaki, M.: Earthquakes as self-organized critical phenomena, *J. Geophys. Res.*, 95, 6853-6860, doi:10.1029/JB095iB05p06853, 1990.
- Juanico, D. E., Longjas, A., Batac, R., and Monterola, C.: Avalanche statistics of granular driven slides in a miniature mound, *Geophys. Res. Lett.*, 35, L19403, doi:10.1029/2008GL035567, 2008.
- 25 Livina, V. N., Havlin, S., and Bunde, A.: Memory in the Occurrence of Earthquakes, *Phys. Rev. Lett.*, 95, 208501, doi:10.1103/PhysRevLett.95.208501, 2005.
- Lübeck, S.: Large-scale simulations of the Zhang sandpile model, *Phys. Rev. E*, 56, 1590-1594, doi:10.1103/PhysRevE.56.1590, 1997.
- Malamud, B. D. and Turcotte, D. L.: Cellular automata models applied to natural hazards, *Comput. Sci. Eng.*, 2, 42-52, doi:10.1109/5992.841795, 2000.
- 30 Olami, Z., Feder, H. J. S., and Christensen, K.: Self-organized criticality in a continuous, nonconservative cellular automaton modeling earthquakes, *Phys. Rev. Lett.*, 68, 1244, doi:10.1103/PhysRevLett.68.1244, 1992.
- Paczuski, M., Boettcher, S., and Baiesi, M.: Interoccurrence Times in the Bak-Tang-Wiesenfeld Sandpile Model: A Comparison with the Observed Statistics of Solar Flares, *Phys. Rev. Lett.*, 95, 181102, doi:10.1103/PhysRevLett.95.181102, 2005.
- Paguirigan Jr., A.A., Monterola, C. and Batac, R. C.: Loss of criticality in the avalanche statistics of sandpiles with dissipative sites, *Commun. Nonlin. Sci. Numer. Simulat.*, 20, 785-793, doi:10.1016/j.cnsns.2014.06.020, 2015.
- 35 Piegari, E., Cataudella, V., Di Maio, R., Milano, L., and Nicodemi, N.: A cellular automaton for the factor of safety field in landslides modeling, *Geophys. Res. Lett.*, 33, L01403, doi:10.1029/2005GL024759, 2006.



- Saichev, A. and Sornette, D.: ‘Universal’ Distribution of Interearthquake Times Explained, *Phys. Rev. Lett.*, 97, 078501, doi:10.1103/PhysRevLett.97.078501, 2006.
- Stacy, S. J., McCloskey, J., and Bean, C. J.: Heterogeneity in a self-organized critical earthquake model, *Geophys. Res. Lett.*, 23, 383-386, doi:10.1029/96GL00257, 1996.
- 5 Touati, S., Naylor, M., and Main, I. G.: Origin and Nonuniversality of the Earthquake Interevent Time Distribution, *Phys. Rev. Lett.*, 102, 168501, doi:10.1103/PhysRevLett.102.168501, 2009.
- Zaliapin, I. and Ben-Zion, Y.: Artefacts of earthquake location errors and short-term incompleteness on seismicity clusters in southern California, *Geophys. J. Int.*, 202, 1949-1968, doi:10.1093/gji/ggv259, 2015.
- Zaliapin, I., Gabrielov, A., Keilis-Borok, V., and Wong, H.: Clustering Analysis of Seismicity and Aftershock Identification, *Phys. Rev. Lett.*, 101, 018501, doi:10.1103/PhysRevLett.101.018501, 2008.
- 10 Zhang, Y.-C.: Scaling theory of self-organized criticality, *Phys. Rev. Lett.*, 63, 47073, doi:10.1103/PhysRevLett.63.470, 1989.